Meas. Sci. Technol. 3 (1992) 384–393. Printed in the UK

Fluorescence decay studies applying a cw femtosecond dye laser pumped ungated inverse time-correlated single photon counting system

W Bäumler, A X Schmalzl, G Gößl and A Penzkofer

Naturwissenschaftliche Fakultät II – Physik, Universität Regensburg, W-8400 Regensburg, Federal Republic of Germany

Received 24 June 1991, in final form 21 October 1991, accepted for publication 11 November 1991

Abstract. An ungated inverse time-correlated single-photon counting system is described. The excitation source is a CW-pumped, linear prism-pair-stabilized, passive mode-locked femtosecond dye laser. The excitation pulse repetition rate is 120 MHz. The sample emission is detected with a microchannel plate photomultiplier tube. An iterative least-squares reconvolution method is applied to the data analysis. The fluorescence lifetimes, the reorientation times and the anisotropy factors of the dye solutions cresyl violet perchlorate and rhodamine 101 perchlorate in ethanol are determined.

1. Introduction

The determination of fluorescence decay curves by time-correlated single-photon counting is well established ([1] and references therein). High repetition rate flashlamps with nanosecond and subnanosecond pulse durations [2], subnanosecond pulsed radiation from synchrotrons and storage rings [3], and picosecond lasers [4] are widely used as excitation sources. Fast photodetectors with low transit time jitter, such as side-on photomultipliers [5], end-on photomultipliers [2, 6], crossed-field photomultipliers [6], microchannel plate photomultipliers [4, 7], and avalanche photodiodes [8], are applied for single-photon signal detection. Powerful deconvolution techniques such as the iterative least-squares reconvolution method [1], the delta function convolution method [9, 10], the instrument response mimic technique [11], Fourier transform analysis [12, 13] and the full-fit convolution method [14] have been developed to resolve fluorescence lifetimes even if they are up to a factor of ten times shorter than the instrument response time [1]. Fluorescence lifetimes down to a few picoseconds have been determined [4, 7, 8, 15].

The data acquisition rate of time-correlated single photon counting systems is limited to about 150 kHz by the conversion period of typically 7 μs of the applied time-to-amplitude converters (TACs). The excitation rate of the fluorescence sample has to be at least a factor of 100 higher than the detection rate of the single-photon counting system in order to be in the single-photon counting regime and to avoid pulse pile-up effects [1]. For excitation rates above 150 kHz, inverse time correlation is the appropriate single-photon counting technique [16], where a fluorescence single-photon signal starts the TAC and a signal derived from the excitation pulse stops the TAC.

For picosecond laser excitation sources, synchronously pumped and cavity dumped dye lasers are most widely used [4, 6, 9, 11]. The cavity dumper reduces the repetition rate. If the temporal pulse separation is made a factor of five to ten times longer than the slowest relaxation rate, then complete de-excitation occurs between the excitation pulses. Generally multi-exponential decay functions are fitted to the fluorescence decay curves in the deconvolutional process [1].

In some reports, the high repetition rate of cw synchronously pumped dye lasers was applied directly to the sample excitation [13, 14, 17–20]. Gating techniques were applied to reduce the trigger pulse rate to the TAC [13, 15, 18, 20, 21]. Ungated operation at high repetition rate was reported in [15–17]. The gating allows the insertion of time delays in the stop line to reduce the start stop interference effects [13, 15, 18, 20, 21]. If the temporal pulse separation becomes comparable to the slowest relaxation rate, then fluorescence accumulation effects have to be considered in the data analysis [12–14].

In this paper, a cw pumped, linear prism-pair stabilized, passive mode-locked femtosecond dye laser with the saturable absorber jet in the middle of the resonator

0957-0233/92/040384+10 $04.50

(colliding-pulse mode-locking position) [22] is used as excitation source with its full repetition rate of 120 MHz. This laser operates very stably. The single-photon counting system is operated in the ungated inverse time-correlation mode. A microchannel plate photomultiplier tube serves as a single-photon detector. The fluorescence contributions from previous excitation pulses are taken into consideration in the fluorescence fit functions. The iterative least-squares reconvolution method is applied. Before, only the Fourier transform analysis [12, 13] and the full-fit convolution method [14] were applied to the data analysis in the case of high repetition rate excitation. The fluorescence lifetimes, molecular reorientation times, and anisotropy factors of the dyes cresyl violet perchlorate (oxazine 9) and rhodamine 101 perchlorate (rhodamine 640) in ethanol are determined at room temperature.

Instead of the linear colliding-pulse mode-locked (CPM) dye laser applied here [22], a conventional ring CPM dye laser [23, 24] or a linear antiresonant ring CPM dye laser [25, 26] could have been used as well. These CW pumped, passive mode-locked, prism-pair stabilized lasers are much less expensive and much simpler to operate (no synchronization length adjustment between active mode-locked pump laser and dye laser) than synchronously pumped and cavity dumped picosecond dye lasers.

2. Experimental

A schematic diagram of the experimental set-up is shown in figure 1. Essentially, it consists of a femtosecond dye laser, a femtosecond pulse diagnostics part, and a single-photon counting arrangement with a trigger and signal branch.

The femtosecond dye laser is pumped by a CW argon ion laser (Spectra-Physics Model 2016 5 W laser, 3 W multi-line pumping including 488 nm and 514.5 nm). A detailed description of the dye laser is given in [22]. In brief, the dye laser has a linear resonator arrangement. It is passive mode-locked and prism-pair stabilized. The gain jet is positioned a quarter resonator distance away from the output mirror for equal amplification of the counter-propagating pulses. The absorber jet is in the middle of the resonator (the middle of the resonator is the CPM position of counter-circulating pulses). In the case of exact positioning of the absorber jet in the middle of the resonator, the counter-circulating pulses pass twice per round-trip through the absorber jet and overlap each time in the absorber jet. If the absorber jet is detuned from the CPM position, the pulses overlap (collide) only once per round-trip in the absorber jet. The intra-cavity prism-pair is adjusted to the negative group velocity dispersion regime where it causes a very stable laser performance independent of an absorber jet detuning from the CPM position [22]. For this prism-pair arrangement, the laser operates in the soliton-like pulse formation regime [22, 26 28] caused by the interaction of positive self-phase modulation [29, 30] and negative group velocity dispersion. The active medium of the laser is rhodamine 6G in ethylene glycol and the saturable absorber is DODCI in ethylene glycol. The laser wavelength is 620 nm, the pulse duration is set to approximately 150 fs by prism-pair positioning, and the average output power is approximately 5 mW. The pulse repetition rate is 120 MHz (resonator round-trip time $t_R = 16.6$ ns, pulse separation $t_S = t_R/2 = 8.3$ ns). A half-waveplate WP rotates the laser polarization to the vertical direction.

For pulse diagnostics, a spectrograph SP1 together with a vidicon system VID measures the laser spectrum, and a rotating mirror intensity autocorrelator [31] monitors the pulse duration.

Trigger pulses of the single-photon counting system are formed by splitting off part of the excitation light. An avalanche photodiode (APD) (Telefunken BPW28, supply voltage 150 V, gain ≈ 150, pulse rise-time ≈ 200 ps, pulse width ≈ 500 ps) is used as trigger detector. The output is amplified in an RF-amplifier A1 (Mini-Circuits Model ZHL-1A, 1 dB flatness region from 2 MHz to 500 MHz, 1 W maximum output power, 16 dB power amplification). The amplified pulses are shaped to NIM pulses in a leading edge discriminator (LED) (Tennelec Model TC454 with leading edge module). The LED output pulse width is set to approximately 10 ns thereby reducing the trigger pulse rate by a factor of two to 60 MHz. Only one stop pulse occurs per round-trip time. Therefore, a slight detuning of the absorber jet of the dye laser out of the CPM position, which causes a slight change of the pulse separation t_S of the counter-propagating pulses (round-trip time t_R remains unchanged; $t_S = t_R/2$ at the CPM position), has no influence on the time resolution of the single-photon counting system. The pulses are properly delayed in a coaxial cable delay box (Ortec Model 425A). The trigger pulses stop the time-to-amplitude conversion after the fluorescence detection branch has started the TAC.

In front of the sample S, the Glan polarizer (GP) transmits vertically polarized light. An interference filter (IF) and an aperture A clean the incident radiation. The sample is filled with either a fluorescent dye for collecting fluorescence decay data or a Rayleigh scattering medium for recording the instrument response function. The scattered light from sample S is collected by lens L1 and directed to the spectrometer SP2 by lens L2. The dichroitic polarizer (DP) is oriented at a magic angle $\theta_m = 54.7°$ relative to the vertical polarization of the input light for the fluorescence lifetime determination [1, 32]. It is turned to the vertical direction and the horizontal direction for the determination of the molecular reorientation time and the anisotropy factor. The spectrometer SP2 separates a wavelength region out of the fluorescence spectrum. The single-photon events are amplified by a factor of approximately 5×10^5 in a microchannel plate photomultiplier (MCP) tube (Hamamatsu R1564-01, 12 μm microchannel diameter). The MCP photomultiplier is separated some distance from the monochromator so that the radiation fills the sensitive area of the detector. The negative MCP photomultiplier output signals are increased in two broadband amplifiers A2 and A3 (Mini Circuits ZHL-1A) before they enter a constant fraction discriminator (CFD) (Tennelec Model 454 with constant

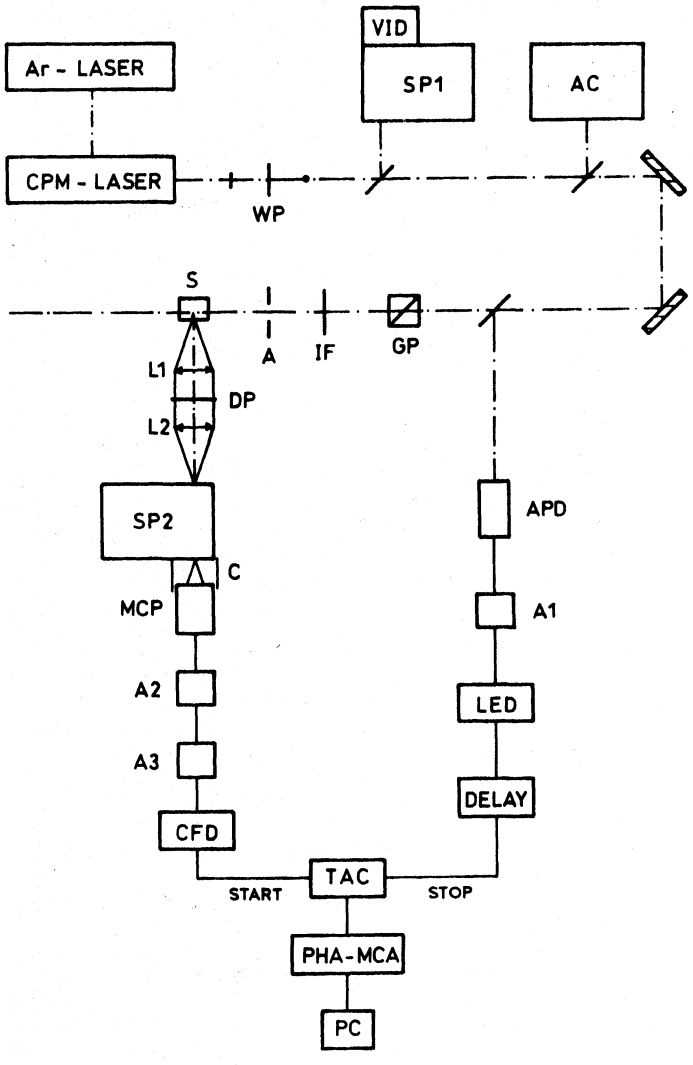

Figure 1. Experimental set-up. SP1, 25 cm grating spectrometer; VID, vidicon; AC, intensity autocorrelator; WP, $\lambda/2$-waveplate; GP, Glan polarizer; DP, dichroitic polarizer; IF, interference filter; A, aperture; S, sample; L1, L2, lenses ($f = 10$ cm); C, cover tube; SP2, 25 cm grating monochromator (slit width = 0.1 mm for cresyl violet, and 0.3 mm for rhodamine 101); MCP, microchannel plate photomultiplier; APD, avalanche photodiode; A1–A3, broadband RF amplifiers; LED, leading edge discriminator; CFD, constant fraction time discriminator; TAC, time-to-amplitude converter; PHA-MCA, pulse height analyser—multichannel analyser; PC, personal computer.

fraction module, attenuation factor $f = 0.2$, maximum repetition rate 200 MHz, internal signal delay set to approximately 500 ps). The output pulses of the CFD start the time-to-amplitude conversion in the biased amplifier TAC (Ortec Model 457). The analogue output voltage signals of the TAC are proportional to the start–stop time interval. They are digitized and stored in a pulse-height analyser multichannel analyser (PHA-MCA) system (Ortec-Norland 5608, 100 MHz, 13 bit ADC, 8192 channels, 2^{20} memory).

3. Data analysis

The experimental signal plots are transferred to background-free and modulation-corrected curves, appropriate fluorescence decay functions are introduced, and the iterative least-squares reconvolution method is applied to extract fluorescence decay parameters by deconvoluting the background-free modulation-corrected fluorescence and instrument response curves.

3.1. Background-free and modulation-corrected data

The experimental fluorescence decay curves $I(t)$ represent convolutions of the true fluorescence curves $G_t(t)$ with the instrument response functions $P(t)$, i.e.

$$I(t) = \int^{t} P(t')G_t(t - t')\,dt'.$$

The instrument response function $P(t)$ for the fluor-

escence measurement is unknown. It is approximated by the signal curve $P_R(t+\delta)$ of a Rayleigh scattering sample. δ is the channel shift increment which takes care of the transit time difference between the fluorescence signal and the Rayleigh scattering signal [1]. In our experiments, we used Ludox CL-X (colloidal silicon dioxide in water from Du Pont, particle size 21 nm) as scattering medium. The background signal $I_b(t)$ (due to thermally released electrons from the photocathode of the MCP photomultiplier) is measured separately (the input light signal is blocked). It is subtracted from the fluorescence curves $I(t)$ and the instrument response curves $P_R(t)$ to yield background-free curves $I_0(t)$ and $P_0(t)$. In addition, the signal modulation behaviour with time [2] is monitored by blocking the laser radiation to the sample and exciting the Rayleigh scatterer with a tungsten lamp. The tungsten lamp signal curve $I_c(t)$ would scatter statistically around a constant value in the absence of amplification modulation. The background-free curves $I_0(t)$ and $P_0(t)$ are corrected to modulation-free conditions by normalizing them to $I_n(t) = I_0(t)\bar{I}_c/I_c(t)$ and $P_n(t) = P_0(t)\bar{I}_c/I_c(t)$ where $\bar{I}_c$ is the time-averaged value of $I_c(t)$.

A typical tungsten lamp curve I_c is plotted against channel number in figure 2(*a*), while in figure 2(*b*) an instrument response function P_R is shown without background subtraction and without modulation correction.

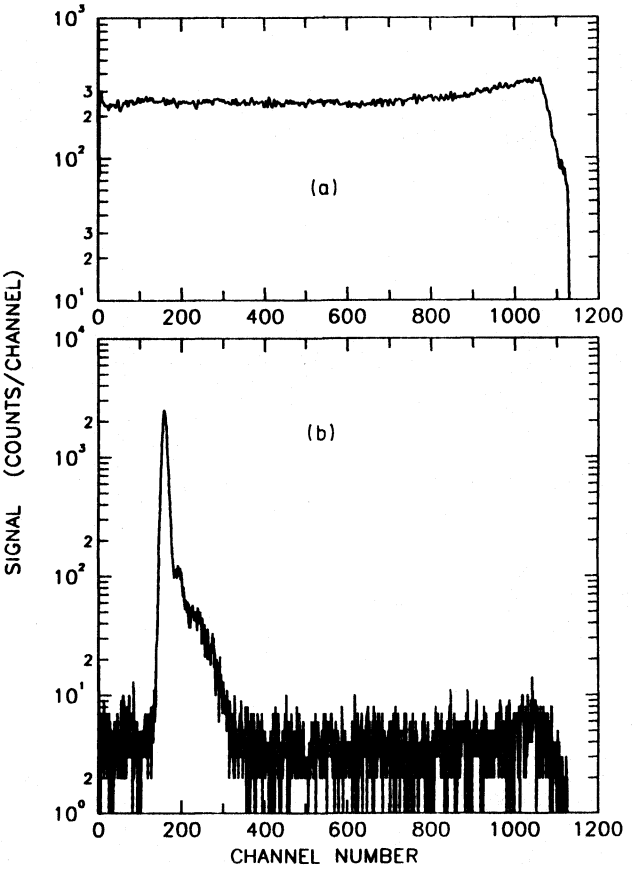

Figure 2. (*a*) A typical tungsten lamp Rayleigh scattering signal distribution $I_c(i)$ used for modulation correction, where i is the channel number and the accumulation time = 1200 s. (*b*) A typical uncorrected instrument response curve $P(i)$. The Rayleigh scatterer is Ludox CL-X; accumulation time = 800 s; time-calibration = 125 channels ns^{-1}; instrument response time = 100 ps (FWHM); total count rate = 58 s^{-1}.

3.2. Fluorescence decay functions

The true fluorescence decay curves $G_t(t)$ are approximated by fit functions $G(t)$ of the form

$$G(t) = \sum_{j=1}^{l} a_{2j-1} g_j(t/a_{2j}) \qquad (1)$$

where the parameters a_{2j-1} give the contributions of the functions g_j to G, and the parameters a_{2j} are the time constants.

In our studies, single exponential fluorescence decay functions and single exponential molecular reorientation functions are appropriate (give good fits). The three situations of:

(i) magic angle detection,
(ii) vertical excitation and vertical detection polarization,
(iii) vertical excitation and horizontal detection polarization

are studied.

In our high repetition rate excitation experiments, population accumulation cannot be neglected [12–14]. The single-pulse-excitation fluorescence decay functions [1, 33] change to the following expressions:

(i) magic angle arrangement

$$G_m(t) = a_{1m} \sum_{k=0}^{\infty} \exp\left[-\frac{t+kt_R}{\tau_F}\right] = a_{1m} \frac{\exp(-t/\tau_F)}{1-\exp(-t_R/\tau_F)} \qquad (2)$$

where t_R is the temporal separation of adjacent pulses and τ_F is the fluorescence lifetime. The fit parameters of equation (2) are a_{1m} and τ_F, where a_{1m} is scaled to unity.

(ii) vertical–vertical arrangement

$$G_v(t) = a_{1v} \sum_{k=0}^{\infty} \left\{ \exp\left[-\frac{t+kt_R}{\tau_F}\right] + 2r_0 \exp\left[-(t+kt_R)\left(\frac{1}{\tau_F}+\frac{1}{\tau_{or}}\right)\right]\right\}$$
$$= a_{1v} \frac{\exp(-t/\tau_F)}{1-\exp(-t_R/\tau_F)} + a_{2v} \frac{\exp(-t/\tau_{eff})}{1-\exp(-t_R/\tau_{eff})} \qquad (3)$$

where r_0 is the fluorescence anisotropy factor [1, 33], τ_{or} is the reorientation time of the excited molecules in the S_1 state and τ_{eff} is given by $\tau_{eff}^{-1} = \tau_F^{-1} + \tau_{or}^{-1}$. The fit parameters of equation (3) are a_{1v}, a_{2v}, and τ_{eff} (τ_F is already known from magic angle measurements). r_0 and τ_{or} are given by

$$r_0 = \frac{a_{2v}}{2a_{1v}} \qquad (4)$$

and

$$\tau_{or} = \frac{\tau_{eff}\tau_F}{\tau_F - \tau_{eff}} \tag{5}$$

(iii) vertical–horizontal arrangement

$$G_h(t) = a_{1h}\sum_{k=0}^{\infty}\left\{\exp\left(-\frac{t+kt_R}{\tau_F}\right) - r_0\exp\left[-(t+kt_R)\left(\frac{1}{\tau_F}+\frac{1}{\tau_{or}}\right)\right]\right\}$$

$$= a_{1h}\frac{\exp(-t/\tau_F)}{1-\exp(-t_R/\tau_F)} + a_{2h}\frac{\exp(-t/\tau_{eff})}{1-\exp(-t_R/\tau_{eff})} \tag{6}$$

with

$$r_0 = -\frac{a_{2h}}{a_{1h}} \tag{7}$$

where τ_{or} is given by equation (5). The fit parameters in equation (6) are a_{1h}, a_{2h} and τ_{eff}.

The fluorescence anisotropy is defined by [1, 34]

$$r(t) = \frac{I_{\parallel}(t) - I_{\perp}(t)}{I_{\parallel}(t) + 2I_{\perp}(t)} = r_0\exp\left[-\frac{t}{\tau_{or}}\right] \tag{8}$$

where $I_{\parallel}$ is the fluorescence component polarized parallel to the excitation light, and $I_{\perp}$ is the fluorescence component polarized perpendicular to the excitation light. r_0 is given by [1, 32, 34]

$$r_0 = \tfrac{1}{5}[3\cos^2(\theta) - 1] \tag{9}$$

where θ is the angle between the absorption and emission transition dipoles. For parallel orientation of the absorption and emission transition dipole moments $r_0 = 0.4$, while for perpendicular orientation of the dipoles $r_0 = -0.2$.

3.3. Least-squares reconvolution method

The iterative least-squares reconvolution method with channel shift [1] is applied to the determination of the fit parameters of the fluorescence decay functions $G(t)$. The method is described in [1]. The data analysis is carried out on a mainframe computer.

The accuracy of the fit is characterized by the reduced chi-squared value χ_v^2 and the weighted residual function $R(t_i)$. Their definitions are given in [1].

For a good fit, χ_v^2 should be in the region between 0.8 and 1.2 [1]. χ_v^2 is improved by increasing the signal count rate and the accumulation time. The weighted residual function $R(t)$ should scatter statistically around zero [1].

4. Results

The described experimental system and the data analysis procedure have been applied to study the fluorescence relaxation kinetics of the organic dyes cresyl violet perchlorate ([33–35] and references therein) and rhodamine 101 perchlorate ([35–37] and references therein) in the solvent ethanol at room temperature (20 °C).

The absorption and stimulated emission cross-section spectra of the investigated dyes are shown in the figures 3 and 4 (own measurement [38]). The structural formulae of the dyes are included in the figures.

The fluorescence decay curves were measured under the following conditions: the excitation wavelength was 620 nm, the detection wavelengths were 620 nm for Ludox CL-X and cresyl violet, and 600 nm for rhodamine 101. The dye concentrations were kept low to avoid fluorescence reabsorption and delayed re-emission. The cell length along the pump laser direction was 1 cm. For cresyl violet (fluorescence maximum at 635 nm), the cell thickness along the detection direction was 1 cm and the transmission at 620 nm was T (1 cm) = 0.84. Rhodamine 101 was excited in the long-wavelength absorption region. The cell thickness along the detection direction was 2 mm and the transmission at 600 nm was T (2 mm) = 0.94 (fluorescence peak at 595 nm).

The fluorescence decay curves of cresyl violet and rhodamine 101 are shown in figures 5–7. The background-free and modulation-corrected fluorescence signals $I_n(t)$ and the corresponding weighted residual functions $R(t)$ are displayed for the magic angle (figure 5), the vertical–vertical (figure 6), and the vertical horizontal arrangements (figure 7). The fit parameters are listed in the figure captions. The fluorescence accumulation by the fast-repetition pulse excitation is clearly seen by the fluorescence signal preceding the step-like signal rise.

Weighted average values of r_0 and τ_{or} are calculated from the vertical vertical (VV) and the vertical horizontal (VH) measurements by

$$\bar{b} = \frac{2b_{vv}|\chi^2_{r,vv} - 1|^{-1} + b_{vh}|\chi^2_{r,vh} - 1|^{-1}}{2|\chi^2_{r,vv} - 1|^{-1} + |\chi^2_{r,vh} - 1|^{-1}} \tag{10}$$

where b stands for r_0 and τ_{or}. The vertical–vertical measurements are weighted by a factor of two since their anisotropic fluorescence contribution is twice as strong as the vertical–horizontal contributions (equations 3 and 6). The factors $|\chi_v^2 - 1|^{-1}$ take care of the fact that measurements with small $(\chi_v^2 - 1)$ values are more reliable.

5. Discussion

The determined fluorescence lifetimes τ_F, reorientation times of the molecules in the S_1 state τ_{or}, and anisotropy factors r_0 are collected in table 1. Our results agree reasonably well with reported data ([33] for cresyl violet, [37] for rhodamine 101). In [39], a rather long fluorescence lifetime of $\tau_F = 5.9$ ns was reported for rhodamine 101 in ethanol. τ_{or} and r_0 of rhodamine 101 perchlorate in ethanol have not been determined previously. A discussion on the deviation of r_0 from the limiting values of $r_0 = 0.4$ for parallel orientation of the absorption and emission transition dipole moments is given in [33, 40, 41].

Table 1. Determined fluorescence spectroscopic data of cresyl violet perchlorate (oxazine 9) and rhodamine 101 perchlorate (rhodamine 640) in ethanol at room temperature.

Parameter	Cresyl violet	Rhodamine 101
τ_f (ns)	3.19 ± 0.1	4.25 ± 0.2
τ_{or} (ps)	358 ± 40	154 ± 20
r_0	0.36 ± 0.02	0.40 ± 0.03

The magic-angle fluorescence decay curves fit well to single-exponential decays. The time constants are accurately determined to be τ_F (cresyl violet) = 3.19 ± 0.1 ns and τ_F (rhodamine 101) = 4.25 ± 0.2 ns. Both dyes are well suited as standards in time-resolved fluorescence decay measurements [42] (calibration of streak cameras [43] and time-correlated single-photon counting systems). They may be applied as reference dyes in single-photon counting data analysis employing the instrument response function mimic technique [11] or the delta function convolution technique [9, 10]

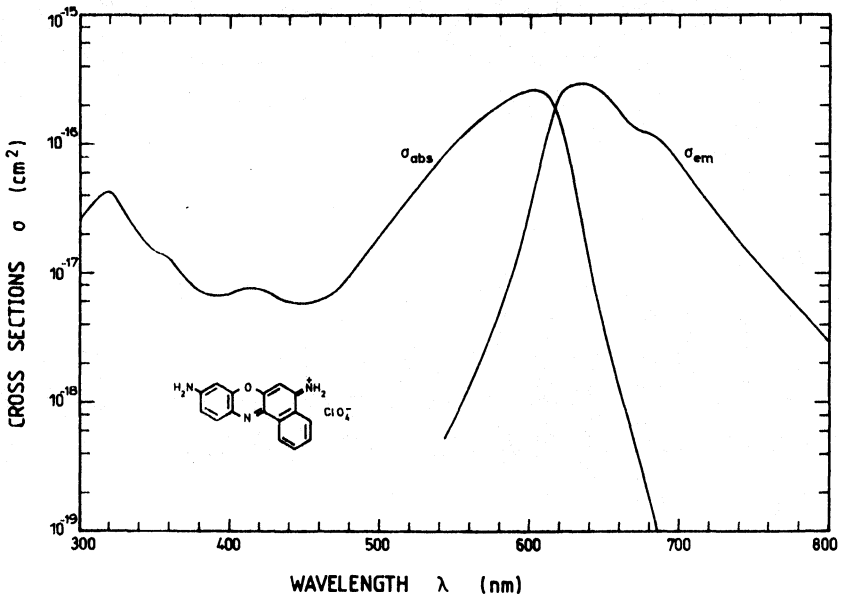

Figure 3. Absorption and stimulated-emission cross-section spectra of cresyl violet perchlorate in ethanol. The structural formula is included.

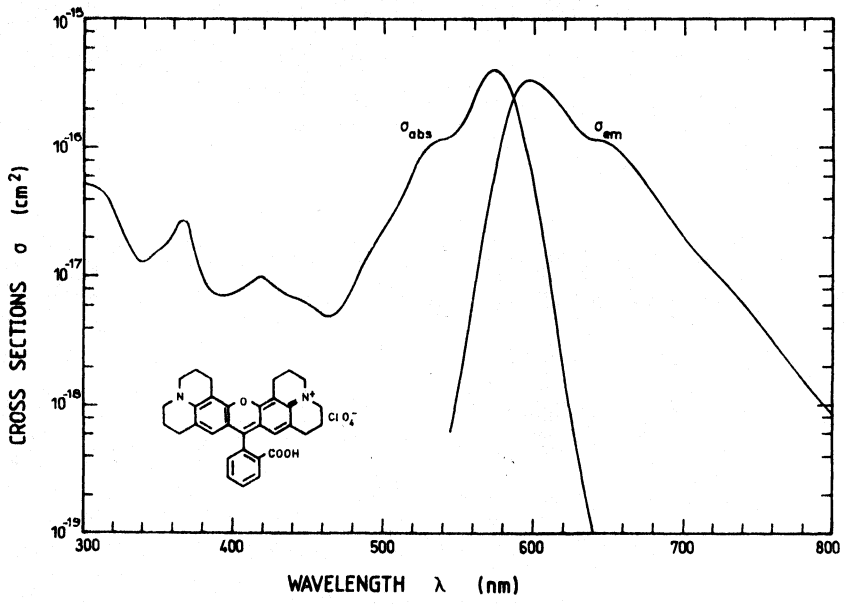

Figure 4. Absorption and stimulated emission cross-section spectra of rhodamine 101 perchlorate in ethanol. The structural formula is included.

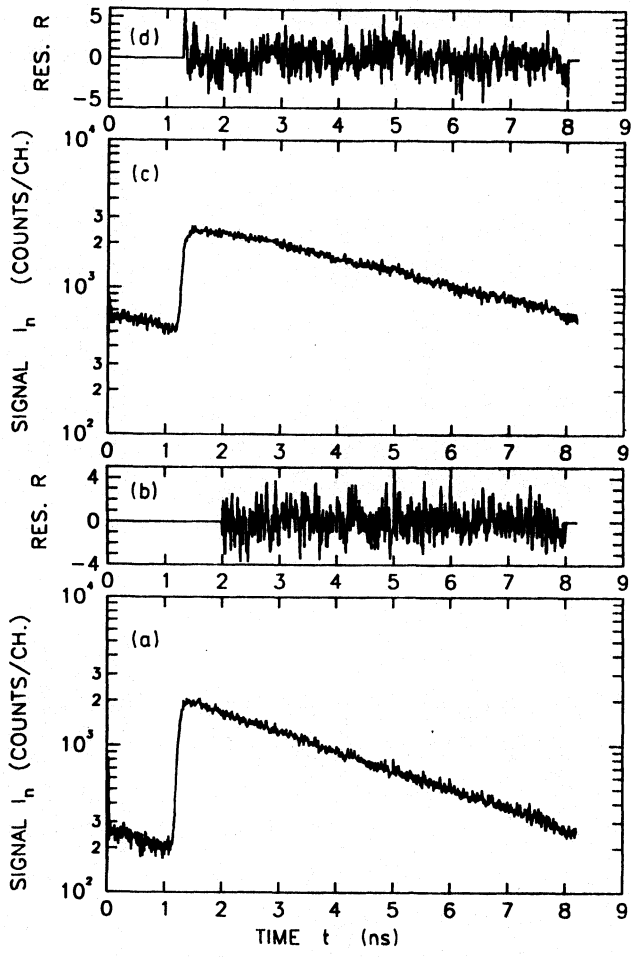

Figure 5. (*a*, *c*) background-free and modulation-corrected fluorescence decay curves $I_n(t)$, and (*b*, *d*) corresponding weighted residual functions $R(t)$ under magic angle excitation-detection conditions. (*a*, *b*) cresyl violet in ethanol: accumulation time = 3000 s; fit parameter $\tau_F = 3187.4$ ps; $\chi_v^2 = 1.721$; total count rate = 270 s^{-1}. (*c*, *d*) rhodamine 101 in ethanol: accumulation time = 4200 s; fit parameter $\tau_F = 4.247$ ns; $\chi_v^2 = 2.476$; total count rate = 330 s^{-1}.

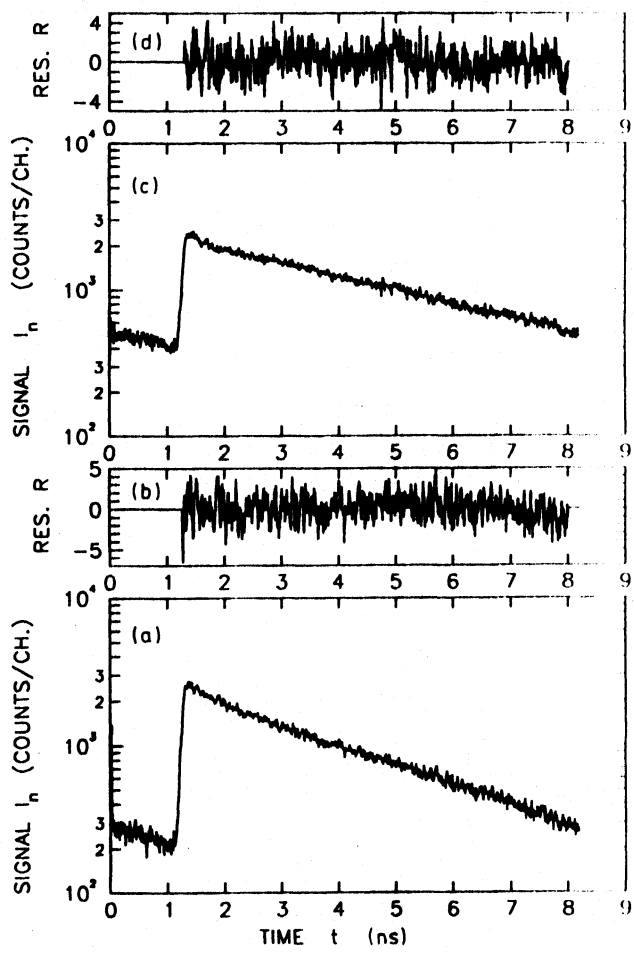

Figure 6. (*a*, *c*) $I_n(t)$ and (*b*, *d*) $R(t)$ for the vertical–vertical excitation-detection arrangement. (*a*, *b*) cresyl violet in ethanol: accumulation time = 2400 s; fit parameters $a_{1v} = 0.00757$, $a_{2v} = 0.00504$, $\tau_{eff} = 291.3$ ps, giving $r_0 = 0.333$, and $\tau_{or} = 321$ ps; $\chi_v^2 = 2.452$; total count rate = 380 s^{-1}. (*c*, *d*) rhodamine 101 in ethanol: accumulation time = 4600 s; fit parameters $a_{1v} = 0.00937$, $a_{2v} = 0.00713$, $\tau_{eff} = 166$ ps, giving $r_0 = 0.38$ and $\tau_{or} = 173$ ps; $\chi_v^2 = 2.04$; total count rate = 245 s^{-1}.

instead of the iterative least-squares reconvolution method. These techniques require the fluorescence decay curve of a reference dye having a single exponential decay instead of the instrument response function.

Rhodamine 101 may be used as a fluorescence standard for excitation wavelengths $\lesssim 600$ nm and fluorescence detection wavelengths between 600 nm and 720 nm (see figure 4). Cresyl violet may be used for excitation wavelengths $\lesssim 630$ nm and emission wavelengths between 620 and 760 nm (see figure 3).

6. Conclusions

An ungated inverse time-correlated single-photon counting system with a 120 MHz femtosecond dye laser excitation source was applied to the fluorescence lifetime, the molecular S_1 state reorientation time, and the fluorescence anisotropy measurement of cresyl violet and rhodamine 101 in ethanol. The iterative least-squares reconvolution method was applied to the extraction of the spectroscopic parameters, taking the fluorescence accumulation effects into account. In the experiment, fluorescence decay curves were measured for magic angle, vertical–vertical, and vertical–horizontal polarization arrangements. It would suffice to use only a vertical–vertical or a vertical–horizontal polarization arrangement to extract the fluorescence lifetime τ_F, the orientation time τ_{or}, and the anisotropy factor r_0 simultaneously by a double-exponential iterative least-squares reconvolution fitting.

The present high repetition rate single-photon counting system with an instrument response function half-width $t_{irf} = 100$ ps and an excitation pulse separation of $t_R = 8.3$ ns is capable of measuring single-exponential fluorescence lifetimes in the range between 5 ps and 40 ns with high accuracy. This fact was checked by an iterative least-squares reconvolution of artificial data [11] where the maximum counts were set to 5000 per channel. Fluorescence lifetimes down to $\tau_F = 1$ ps should be

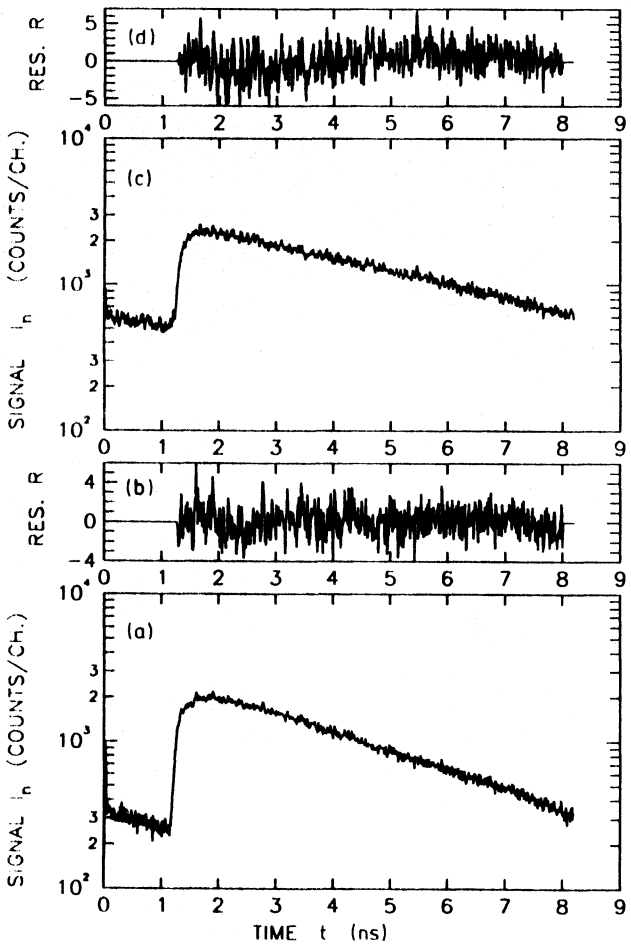

Figure 7. (*a*, *c*) $I_n(t)$ and (*b*, *d*) $R(t)$ for the vertical–horizontal excitation-detection arrangement. (*a*, *b*) cresyl violet in ethanol: accumulation time = 3000 s; fit parameters $a_{1n} = 0.00900$, $a_{2n} = -0.00348$, $\tau_{eff} = 356.9$ ps, giving $r_0 = 0.386$, and $\tau_{or} = 402$ ps; $\chi^2_v = 1.861$; total count rate = 323 s^{-1}. (*c*, *d*) rhodamine 101 in ethanol: accumulation time = 6000 s; fit parameters $a_{1n} = 0.00875$, $a_{2n} = -0.00429$, $\tau_{eff} = 54.1$ ps, giving $r_0 = 0.49$, and $\tau_{or} = 55$ ps; $\chi^2_v = 3.761$; total count rate = 222 s^{-1}.

accurately measurable with the described system if a state-of-the-art microchannel plate photomultiplier (Hamamatsu R2809 with 6 μm channel diameters) were used which gives instrument response function half-widths below 30 ps ($t_{Irf} = 28.1$ ps [7], 25 ps [44], 10 ps [45]).

Besides ungated inverse time-correlated single-photon counting measurements, gated inverse time-correlated single photon counting studies were performed. In the latter case, an output signal derived from the CFD of the fluorescence detection branch was applied to gate the fast comparator SP9687 [46] of the LED of the trigger branch (an electronic modification of the gate channel of the Tennelec 454 quadrupole discriminator was necessary for this purpose). The signal modulation behaviour $I_c(t)$ was somewhat worse for the gated system. Otherwise, the performance data of the gated version are similar to the performance data of the ungated version. The ungated version has the advantage that no modifications of the commercial discriminator are necessary.

In our experiments, the counting rate capability of the system of 150 kHz was not exploited (our counting rate was approximately 300 Hz) because of the small average power of the femtosecond laser and the weak light absorption in the fluorescence sample. The count rate could have been increased by widening the spectrometer slit width and lowering the threshold level of the constant fraction discriminator at the cost of slightly broadening the halfwidth of the instrument response function.

The experiments show that CW pumped femtosecond laser (linear arrangement as used here [22], ring CPM laser arrangements [23, 24], or anti-resonant ring CPM systems [25, 26]) can be applied to time-correlated single-photon counting measurements as well as the much more expensive synchronously pumped and cavity dumped laser systems. The excitation wavelength region of the CW pumped femtosecond dye lasers may be adjusted between approximately 490 nm and 900 nm by application of various amplifying dye–saturable absorber combinations (see [26, 47, 48] for reviews). CW pumped, frequency tunable, mode-locked femtosecond Ti:sapphire lasers may be applied in the near infrared spectral region (730 nm to 990 nm) while their second-harmonic light may be used in the blue spectral region (365 nm to 495 nm) [49–51].

The femtosecond pulse durations of the excitation lasers have not yet an advantage compared with the excitation pulse duration of a few picoseconds of synchronously pumped lasers as long as the transit time jitter of the single photon counting detectors and the timing jitter of the electronics are still in the tens of picoseconds region [4, 7, 8, 44, 45].

Acknowledgments

The authors would like to thank the Deutsche Forschungsgemeinschaft for financial support and the Rechenzentrum of the Universität Regensburg for the allocation of computer time.

References

[1] O'Connor D V and Phillips D 1984 *Time-Correlated Single Photon Counting* (London: Academic Press)

[2] Birch D J S, Hungerford G, Nadolski B, Imhof R E and Dutch A D 1988 Time-correlated single-photon counting fluorescence decay studies at 930 nm using spark source excitation *J. Phys. E: Sci. Instrum.* **21** 857–62

[3] Kan'no K, Tanaka K, Kosaka H, Mukai T, Itoh M, Miyanaga T, Fukui K and Watanabe M 1990 Decay time measurements of intrinsic luminescence in alkali halides using single-bunched light pulses from UVSOR *Phys. Scr.* **41** 120–3

[4] Murav T, Yamazaki I and Yoshihara K 1982 Application of a microchannel plate photomultiplier

to the time-correlated photon counting technique *Appl. Opt.* **21** 2297–8
[5] Meister E C, Wild U P, Klein-Bölting P and Holzwarth A R 1988 Time response of small side-on photomultiplier tubes in time-correlated single-photon counting measurements *Rev. Sci. Instrum.* **59** 499–501
[6] Bebelaar D 1986 Time response of various types of photomultipliers and its wavelength dependence in time-correlated single-photon counting with an ultimate resolution of 47 ps FWHM *Rev. Sci. Instrum.* **57** 1116–25
[7] Kume H, Koyama K, Nakatsugawa K, Suzuki S and Fallowitz D 1988 Ultrafast microchannel plate photomultipliers *Appl. Opt.* **27** 1170–8
[8] Cova S, Lacaita A, Ghioni M, Ripamonti G and Louis T A 1989 20-ps timing resolution with single-photon avalanche diodes *Rev. Sci. Instrum.* **60** 1104–10
[9] Wijnaendts van Resandt R W, Vogel R H and Provencher S W 1982 Double beam fluorescence lifetime spectrometer with subnanosecond resolution: Application to aqueous triptophan *Rev. Sci. Instrum.* **53** 1392–7
[10] Boens N, Ameloot M, Yamazaki I, and De Schryver F C 1988 On the use and the performance of the delta function convolution method for the estimation of fluorescence decay parameters *Chem. Phys.* **121** 73–86
[11] James D R, Demmer D R M, Verrall R E and Steer R P 1983 Excitation pulse-shape mimic technique for improving picosecond-laser-excited time-correlated single-photon counting deconvolutions *Rev. Sci. Instrum.* **54** 1121–30
[12] Wild U P, Holzwarth A R and Good H P 1978 Measurement and analysis of fluorescence decay curves *Rev. Sci. Instrum.* **48** 1621–7
[13] Canonica S and Wild U P 1985 Single photon counting with synchronously pumped dye laser excitation *Anal. Instrum.* **14** 331–57
[14] Sakai Y and Hirrayama S 1988 A fast deconvolution method to analyse fluorescence decays when the excitation pulse repetition period is less than the decay times *J. Lumin.* **39** 145–51
[15] Turko B T, Nairn J A and Sauer K 1983 Single photon timing system for picosecond fluorescence lifetime measurements *Rev. Sci. Instrum.* **54** 118–20
[16] Haugen G R, Wallin B W and Lytle F E 1979 Optimization of data-acquisition rates in time-correlated single-photon fluorimetry *Rev. Sci. Instrum.* **50** 64–72
[17] Kinoshita S, Ohta H and Kushida T 1981 Subnanosecond fluorescence-lifetime measuring system using single photon counting method with mode-locked laser excitation *Rev. Sci. Instrum.* **52** 572–5
[18] Alfano A J, Fong F K and Lytle F E 1983 High repetition rate subnanosecond gated photon counting *Rev. Sci. Instrum.* **54** 967–72
[19] Holzwarth A R, Wendler J and Haehnel W 1985 Time-resolved picosecond fluorescence spectra of the antenna chlorophylls in Chlorella vulgaris. Resolution of photosystem I fluorescence *Biochim. Biophys. Acta* **807** 155–67
[20] Cova S and Ripamonti G 1989 Picosecond synchronisation on mode-locked laser pulses by double constant-fraction triggering *Electron. Lett.* **25** 11–2
[21] Louis T A, Ripamonti G and Lacaito A 1990 Photoluminescence lifetime microscope spectrometer based on time-correlated single-photon counting with an avalanche diode detector *Rev. Sci. Instrum.* **61** 11–22
[22] Bäumler W and Penzkofer A 1992 Femtosecond pulse generation in a linear passive mode-locked dye laser *Opt. Quant. Electron.* **24** to be published
[23] Fork R L, Greene B I and Shank C V 1981 Generation of Optical Pulses Shorter than 0.1 psec by Colliding Pulse Mode Locking *Appl. Phys. Lett.* **38** 671–2
[24] Valdmanis J A, Fork R L and Gordon J P 1985 Generation of Optical Pulses as Short as 27 Femtoseconds Directly from a Laser Balancing Self-Phase Modulation, Group-Velocity Dispersion, Saturable Absorption, and Saturable Gain *Opt. Lett.* **10** 131–33
[25] Vanherzeele H, Diels J-C and Torti R 1984 Tunable Passive Colliding-Pulse Mode Locking in a Linear Dye Laser *Opt. Lett.* **9** 549–51
[26] Diels J C 1990 Femtosecond Dye Lasers *Dye Laser Principles with Applications* eds F J Duarte and L W Hillman (San Diego: Academic) ch 3 pp 41–132
[27] Martinez O E, Fork R L and Gordon J P 1985 Theory of Passively Mode-Locked Lasers for the Case of a Nonlinear Complex-Propagation Coeffient *J. Opt. Soc. Am.* B **2** 753–60
[28] Hasegawa A 1990 *Optical Solutions in Fibers*, 2nd edn (Berlin: Springer-Verlag)
[29] Penzkofer A and Bäumler W 1991 Theoretical Analysis of Pulse Development in a Colliding Pulse Mode-Locked Dye Laser *Opt. Quant. Electron.* **21** 727–54
[30] Penzkofer A 1991 Theoretical Analysis of Pulse Shaping of Self-Phase Modulated Pulses in a Grating Pair Compressor *Opt. Quant. Electron.* **23** 685–702
[31] Yasa Z A and Amer N M 1981 A Rapid-Scanning Autocorrelation Scheme for Continuous Monitoring of Picosecond Laser Pulses *Opt. Commun.* **36** 406–8
[32] Cehelnik E D, Mielenz K D and Velapoldi R A 1975 Polarization effects on fluorescence measurements *J. Res. NBS* A **79** 1–15
[33] Dutt G B, Doraiswamy S, Periasamy N and Venkataraman B 1990 Rotational reorientation dynamics of polar dye molecular probes by picosecond laser spectroscopic technique *J. Chem. Phys.* **93** 8498–513
[34] Fleming R G 1986 Chemical Applications of Ultrafast Spectroscopy (New York: Oxford University Press)
[35] Eaton D F 1986 IUPAC Commission on photochemistry: Reference compounds for fluorescence measurements *EPA Newsletter* **28** 21–31
[36] Johansson L B-Å 1990 Limiting fluorescence anisotropies of perylene and xanthene derivatives *J. Chem. Soc. Faraday Trans.* **86** 2103–7
[37] Frank A J, Otvos J W and Calvin M 1979 Quenching of rhodamine 101 emission in methanol and colloidal suspension of latex particles *J. Phys. Chem.* **83** 716–22
[38] Penzkofer A and Leupacher W 1987 Fluorescence behaviour of highly concentrated rhodamine 6G solutions *J. Lumin.* **37** 61–72
[39] Hou Y, Ning C J, Zhou D and Wang W 1987 Fluorescence lifetimes of some laser dyes *Yingyong Huaxue* **4** 53–7
[40] Penzkofer A and Falkenstein W 1976 Photoinduced dichroism and vibronic relaxation of rhodamine dyes *Chem. Phys. Lett.* **44** 547–52
[41] Kawski A, Kubicki A, Weyna I and Janić I 1985 Temperature dependence of limiting fluorescence anisotropy of POPOP in cellulose acetate film *Z. Naturf.* **40a** 559–61
[42] Lampert R A, Chewter L A, Phillips D, O'Connor D V, Roberts A J and Meech S R 1983 Standards for nanosecond fluorescence decay time measurements *Anal. Chem.* **55** 68–73
[43] Minami T and Hirayama S 1990 High Quality Fluorescence Decay Curves and Lifetime Imaging

using an Elliptical Scan Streak Camera *J. Photochem. Photobiol.* A **53** 11–21

[44] Hu Cojen, Motyko A L and Topp M R 1989 Picosecond time-resolved $S_2 \rightarrow S_0$ fluorescence of xanthione in different fluid solvents *Chem. Phys. Lett.* **158** 51–9

[45] Okada T, Nishikawa S, Kanaji K and Mataga N 1990 Dynamics of intramolecular electron transfer in polar solvents *Ultrafast Phenomena VII (Springer Series in Chemical Physics* **53**) (Berlin: Springer) eds C B Harris, E P Ippen, G A Mourou and A H Zewail (Berlin, Heidelberg: Springer) pp 397–401

[46] *Data Converters & Voltage References IC Handbook PS 1989* 1989 (Irvine, CA: Plessey Semiconductors Company) pp 36–40

[47] Penzkofer A 1988 Passive Q-Switching and Mode-Locking for the Generation of Nanosecond to Femtosecond Pulses *Appl. Phys.* B **46** 43–60

[48] French P M W, Williams J A R and Taylor J R 1987 Passively Mode Locked cw Dye Lasers Operating from 490 nm to 800 nm *Revue Phys. Appl.* **22** 1651–1655

[49] Spence D E, Kean P N and Sibbett W 1991 60-fsec Pulse Generation from a Self-Mode-Locked Ti:Sapphire Laser *Opt. Lett.* **16** 42–4

[50] Naganuma K and Mogi K 1991 50 fs Pulse Generation Directly from a Colliding-Pulse Mode-Locked Ti:Sapphire Laser Using an Antiresonant Ring Mirror *Opt. Lett.* **16** 738–40

[51] Keller U, 't Hooft G W, Knox W H and Cunningham J E 1991 Femtosecond Pulses from a Continuously Self-Starting Passively Mode-Locked Ti:Sapphire Laser *Opt. Lett.* **16** 1022–4